DOI Link: https://doi.org/10.61586/SuOws
Vol.65, Issue.10, Part.1, Oct 2025, PP.134-150

Biofabrication of silver nanoparticles and their promising anti-inflammatory and antiarthritic activity for reducing cartilage destruction in joints for bone regeneration and fracture treatment applications

Xiaohua Li[1,a], Yifei Shen[2,3,b*]

[1]*School of Physical Education, Hunan University of Arts and Science, Changde 415000, Hunan, China*

[2]*College of Education of Jilin International Studies University, Changchun 130117, Jilin, China*

[3]*College of Human Sciences of Assumption University, Bangkok 10240, Thailand*

[a]*Email: xhua8@huas.edu.cn*
[b]*Email: yangchunping@jisu.edu.cn*

[*]***Corresponding Author***: Yifei Shen, College of Education of Jilin International Studies University, Changchun 130117, Jilin, China; E-mail:yangchunping@jisu.edu.cn

Received Feb 2025 Accepted Sep 2025 Published Oct 2025

Abstract

In this study, silver nanoparticles (AgNPs) were successfully synthesized by reducing Ag^+ ions using the leaf extract of *Salvia spinosa*, which served as both a capping and reducing agent, with $AgNO_3$ as the precursor. The primary objective was to fabricate AgNPs with enhanced antibacterial efficacy and reduced toxicity. Characterization of the synthesized AgNPs was conducted using Energy Dispersive X-ray Spectrometry (EDX), UV–Visible Spectroscopy (UV-Vis), Fourier Transform Infrared Spectroscopy (FT-IR), X-ray Diffraction (XRD), and Transmission Electron Microscopy (TEM). Furthermore, the antiarthritic potential of AgNPs was evaluated in a collagen-induced arthritis (CIA) animal model, focusing on their ability to mitigate oxidative stress and inflammatory mediators. Treatment with AgNPs resulted in a significant reduction in elevated levels of inflammatory markers such as NF-κB, COX-2, TNF-α, and IL-1β in CIA-induced rats. The nanoparticles also restored the balance between oxidants and antioxidants, bringing levels closer to normal. Biochemical analysis revealed that mRNA expression of NF-κB, TNF-α, iNOS, and COX-2 was upregulated in CIA rats but markedly downregulated following AgNP treatment. These molecular findings were corroborated by histological examination of joint tissues, which showed reduced inflammation and bone erosion in treated animals. Overall, this work demonstrates the therapeutic potential of AgNPs in alleviating oxidative stress and inflammatory responses in CIA, suggesting their promising application in joint repair and arthritis management.

Keywords: AgNPs, joints, cartilage, polyphenols

Introduction

Rheumatoid Arthritis (RA) is termed as a systemic infectious illness and autoimmune categorized by infiltration of multiple immune proteins in the central joint synovial membrane accompanied by pronounced tumors such as pannus development owing to synovium activation and proliferation contributing to oedema, chronic inflammation, discomfort and ultimately leading to joint death in individuals with defined RA. These stimulated synoviocytes (native joint macrophages) are accountable for releasing various inflammatory toxic mediators like interleukin-1b (IL-1b), IL-6, tumor necrosis factor-a (TNF-a), and reactive nitrogen/oxygen organisms (RNS / ROS). Free radicals, RNS/ROS constituting unpaired atoms extracted from molecular nitrogen/oxygen and they are poisonous to cellular elements like DNA, proteins and membrane lipids, resulting in considerable injury to structures of cell and cumulating into a scenario recognized as oxidative stress. This kind of infectious mediators and RNS/ROS in RA are the major regulators of joint failure as well as inflammation [1–3]. These cytokines behave synergistically and stimulate the development of Matrix Metalloproteinases (MMPs) from fragments of extracellular matrix and triggered synoviocytes, a hallmark of arthritis [4]. Transcription receptor NF-kB regulates the expression of these MMPs and noxious inflammatory intermediates [5, 6].

Transcription factor, NF-kB regulates the expression of several genes engaged in inflammatory reactions and intensely modulates their function through multiple stimuli like UV light, oxidative stress and pro-inflammatory cytokines [7]. Furthermore, an appropriate therapeutic approach for RA could be the down-regulation of NF-kB as well as pro-inflammatory cytokines. There is no sustained remedy accessible for RA as of now. The present method of medication provides only symptomatic relief from inflammation and pain.

The current treatment methods for RA include disease-altering anti-rheumatic medications (DAARMs), which are Non-Steroidal Anti-Inflammatory medicines (NSAIMs). The frequently used drug as DAARMs is Methotrexate (MTX), which is often authorized for RA therapy as a primary-line medication. MTX, often a folate analog designed to prevent reductase dihydrofolate and obstruct the prerequisite for cell proliferation, the synthesis of RNA and DNA [8]. In RA, it synthesizes, inhibits and proliferates lymphocytes and other enzymes that are responsible for joint inflammation [9]. Although the utilization of MTX / NSAIMs or DMARMs is only efficient for a really short time, long term implementation creates countless life-threatening side effects like immunosuppression and stomatitis of gastric ulcer [10, 11]. Researchers are therefore attempting to monitor fresh manmade or artificial organic components that cause higher efficiency and lower toxicity for inhibiting inflammation.

Nanotechnology is currently receiving a lot of attention due to its extensive implementation in information technology, energy management, and medicines as well as in electronics [12]. Nanoscale-level materials are produced by precise engineering with regulated physicochemical characteristics, also includes improved

ratio of surface-to-volume, and a large percentage of exposed surface atoms [13]. The discovery of inorganic medicinal nanoparticles (NPs) has a deep effect on the biological sciences. Yet not much research is reported to disclose their utilization in treating rheumatic disease [14, 15]. Metal NPs were being widely studied in biomedical implementations and have an incredibly broad range of uses [16–18]. It includes, in specific, genomics, clinical chemistry, proteineomics [19], immunoanalysis [20], cancer cells and microorganisms detection and photo thermolysis [21–23]. In addition, it is utilized in the optical bioimaging, targeted delivery of medicines, antigens and DNA, as well as tissues and cells scrutinizing with the help of modern approaches [24–26]. Metal nanoparticles have emerged as versatile agents in clinical applications, including diagnostics, prevention, hygiene, and therapy. Among them, gold-based compounds have been used in chrysotherapy for treating arthritis, with therapeutic effects likely attributed to the localized release of metal ions into adjacent connective tissues. Silver (Ag), known for its potent antimicrobial and anti-inflammatory properties, holds promise for developing a new class of anti-arthritic agents that offer higher efficacy and fewer side effects. Despite the broad biomedical use of metal NPs, there is limited scientific evidence supporting the application of silver nanoparticles (AgNPs) in the treatment of rheumatoid arthritis (RA) [27, 28].

The primary goal of this study is to investigate the therapeutic potential of biofabricated AgNPs synthesized using *Salvia spinosa* leaf extract in a collagen-induced arthritis (CIA) rat model. This model closely mimics the histopathological and clinical features of human RA. The study aims to evaluate the anti-inflammatory and antioxidant effects of AgNPs, and their ability to modulate key molecular markers involved in RA pathogenesis.

Materials and Methods

Synthesis of AgNPs

For fabricating AgNPs, 10 mL leaf extract of *Salvia spinosa* was drop wise added at a frequency of about 1 drop/second on a magnetic stirrer to 1 mM $AgNO_3$ of 100 mL solution under steady stirring conditions. The mixture was constantly stirred for about an hour, and then, kept stand still for about a day at a temperature of 25 ºC. The shift in color to reddish yellow from gray confirmed the Ag^+ ions reduction to Ag°. Then, the resultant mixture was centrifuged for about 10 minutes at 10,000 rpm, followed by washing the precipitate with deionized water and repeatedly centrifuging in order to eliminate the impurities. The resultant precipitate was dried overnight at a temperature of 60 °C, which later placed for further study in a desiccator.

Test animals

Male rats of Wistar albino were acquired from Shanghai SLAC Laboratory for Animals, China. Rats were permitted for a week to habituate before the experiment was initiated. All the animals were blindly separated into 4 groups and stored under normal operating surroundings (14:10 hour light: dark ratio, 22 ±

2 °C ambient temperature, 40–45 percent moisture). Water and food were given Ad libitum. In accordance with the guidelines of animal ethics committee, the rats of all groups got humanitarian treatment. The Committee of Institutional Animal Ethics endorsed the testing procedure. Throughout the experiment, all the rats were held under surveillance for water and food consumption, functioning, body weight, etc.

Induction of arthritis

As demonstrated in one of the earlier reports, Collagen form II (CII) immunization, emulsified with Total Freund's Adjuvant (CFA) are the causes of arthritis in Wistar male rats [29]. Briefly, by stirring gently at 4 °C overnight and emulsifying with CFA, collagen was dissipated in 0.1 M acetic acid (2 mg / ml). Every rat was subjected to immunization using subcutaneous injection at the tail's base using 0.2 ml emulsion (200 µg), and the booster dosage was administered after 2 weeks of immunization to ease the signs of the disease.

Evaluation of footpad thickness and arthritic index (AI)

The growth of arthritis was tracked by a separate blind participant without any understanding of the therapy protocol through a four-legged macroscopic scoring apparatus varying from zero to 15 (one score for every red or swollen toe, one score for knuckle or middle-foot digit and five scores for a swollen knee). Added the results of 4 paws and regarded a complete rating of 60 per animal as an induction of RA [30]. Clinical seriousness was also evaluated using a dial-gage caliper to measure footpad density.

Grouping of animals

All the rats are blindly separated into 4 groups with 6 rats in each group. Treatment for all the groups was continued for a period of 20 days by initiating on the 25th day. Group I was considered as control group and was treated with non-induced plus normal saline. The 2nd group was administrated with induced plus normal Saline. The 3rd group was treated with induced plus MTX of 0.25 mg / kg b.w intraperitoneally one time in 7 days. Group IV was administrated with induced plus nanogold of 20 lg/kg b.w intraperitoneally every day throughout the 20 days. The amount of dose to be injected was chosen based on the preliminary study in our lab.

Collection of samples

Rats were overnight fasted after completing the treatment and blood samples were obtained for biochemical analyses through puncturing the retro-orbital vein. Serum has been isolated and utilized for estimating the reduced glutathione, lipid peroxidation, cytokines, cyclooxygenase-2 (COX-2) and NF-kB.

Oxidative stress parameters assessment

Serum can be utilized to determine the lipid peroxidation (LPO) as demonstrated in an earlier report [31]. In brief, serum of 0.5 ml was initially dissolved with Trichloroacetic acid of 20 percent and then the resultant mixture was subjected in thiobarbituric acid (0.07% in sodium sulfate 1 M) and 0.05 N sulphuric acid. The resultant sample was incubated in a hot water tub for about half

an hour, resulting in the formation of MDA-TBA adduct that was extracted further with butanol. The spectrophotometric measurement of LPO was evaluated at about 532 nm and the responses were represented in nM/ml.

As per the earlier described procedure [32], the content of reduced glutathione (GSH) has been estimated in the entire blood. Briefly, the reaction solution of 1 ml included with NADPH [0.2 mM / ml in EDTA phosphate buffer 0.01 M / 0.005 M of 7.5 pH], glutathione reductase (1 unit) and hemolysate of 25 ml. Following the Ellman's reagent (DTNB) addition, determined at 412 nm, a chromophoric product was developed. The result has been represented as lM / ml blood.

Assessment of cytokine levels

The cytokine levels IL-1β and TNF-α in serum were defined by conventional ELISA kits (Pierce Biotechnology, Rockford, IL) utilizing microplate reader, Thermo Scientific, Shanghai, China, as instructed by the manufacturer.

Evaluation of COX-2 and NF-kB levels

Conventional ELISA kits (MyBiosource, CA and Cusa Biotech, Hubei Province, China) were used to measure the COX-2 and NF-kB levels in serum utilizing microplate reader.

Extracting RNA and quantitative real time PCR of animal joints

mRNA levels of NF-kB, TNF-α, inducible nitric oxide synthase (iNOS) and COX-2 were examined in rat joint tissue with the help of qPCR in order to compare the mRNA expression in each group. In short, synovial tissues are separated after rat euthanization as demonstrated in an earlier report [33], then, stored in Trizol overnight for RNA isolation as per the protocol of the manufacturer. NanoDrop (Thermo Scientific, Wilmington, DE) was used to determine the concentration of extracted RNA in nuclease-free water. The RNA purity was evaluated by taking 260/230 and 260/280 nm absorbance ration. The integrity of RNA was analyzed with the help of agarose gel electrophoresis.

RNA of 1 μg from individual joints of each rat from each group was utilized for the generation and amplification of single-stranded cDNA with the help of Verso cDNA fabrication Kit (Thermo Scientific, Shanghai, China). This is further utilized to evaluate the levels of mRNA like COX-2, TNF-α, iNOS and NF-kB utilizing qPCR. As an internal control, glyceraldehyde 3-phosphate dehydrogenase (GAPDH) has been utilized.

Qiagen Thermal Cycler (system of Rotor-Gene Q 5plex HRM from Qiagen) was utilized to perform the real-time PCR. Amplifying responses were accomplished with the help of Maxima SYBR Green / ROX qPCR Master Mix (2×) suite (Thermo Scientific, Shanghai, China) as per the protocol of the manufacturer. Briefly, qPCR was performed with a complete resultant solution of 25 ml, consisting of 0.9 μM primer of 1 μl (forth and back), 1 – 2 μl ⩽ 500 ng cDNA, nuclease-free water and 12.5 μl mixture of maxima SYBR Green master. Initially, denaturation was performed for 5 minutes at a temperature of 95 ° C following with 40 cycles of PCR in 3 steps (at first denaturation, annealing and finally extension for about 15, 30 and 30 seconds at temperatures of 95, 60 and 72 ° C, respectively). Threshold cycle (Ct) was utilized to quantify the PCR products,

which were evaluated by calculating their enhanced fluorescence caused because of the SYBR Green I Dye binding to dsDNA. The earlier reported process, 2^{-}Ct procedure was utilized to calculate the expression of relative change in fold of TNF-α, NF-kB, mRNA and iNOS [34]. The outcomes were standardized to the GAPDH mRNA expression levels in every sample.

Histological studies

Tissues of the rat joints were drawn from CO_2 euthanized rats for histological analysis and then subjected in formalin buffer of 10% followed by decalcification with 10% solution of EDTA. Samples are processed post decalcification, sliced into segments of 3–4 mm wide, followed by staining with eosin and haematoxyl. Any kind of modifications were assessed with the help of 0–4 point scale based on the histological parameters such as pannus development, inflammation and cartilage development. Pannus formation=3, Inflammatory cell infiltration=1, Normal=0, synovium hyperplasia=2 and bone erosion and severe cartilage =4.

Statistical analysis

All the data was represented as median ± SD. Statistical information was examined with the help of one-way ANOVA utilizing SPSS version 16 statistical program (SPSS, Shanghai, China) and individual treatment comparisons were gained through Tukey's multiple comparison test. A statistically significant difference of $p < 0.05$ was taken as important.

Results

Characterization of AgNPs

The analysis of UV-Vis spectra primarily confirmed the synthesis of AgNPs from the reduction of Ag^{+} ions. Due to surface plasma resonance, AgNPs were described to display UV–Vis absorption maxima at 400–500 nm of wavelength range [35]. In this work, after 1 h of the reaction, an absorption peak was noticed at 450 nm showing the development of crystalline AgNPs as represented in Fig. 1 [35]. Furthermore, an intense peak was noticed at 450 nm in commercial AgNPs.

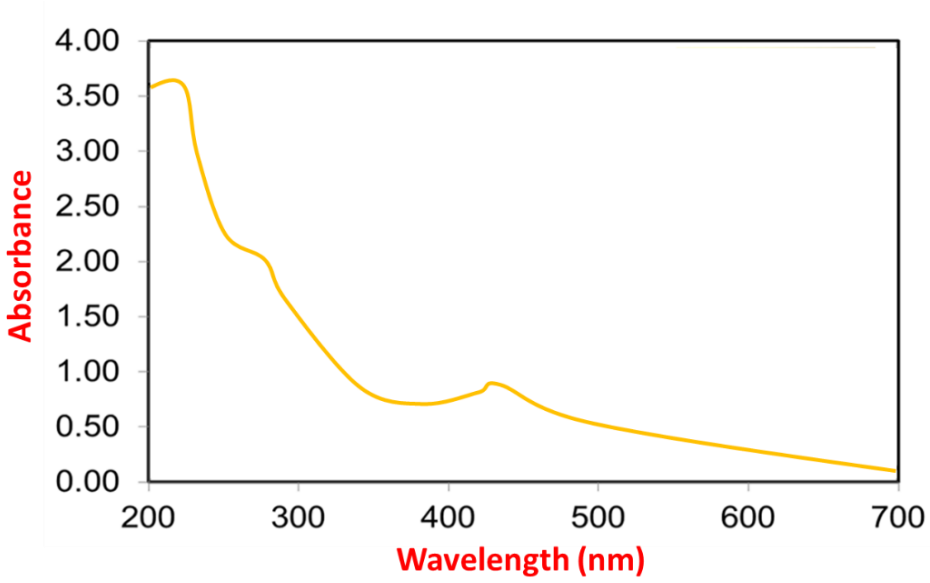

Fig.1. UV-Visible absorption of AgNPs

The indication of strong peak in the EDX examination confirmed the formation of elemental Ag in high percentile as displayed in Fig. 2. Furthermore, a few weak peaks were also discovered in silver nanoparticles indicating carbon and oxygen particles. XRD analysis was carried out to characterize the AgNPs ' solid phase microstructure and crystallinity at 35 ° –85 ° (2θ) scanning range (Fig. 3). About five unique peaks of diffraction were noticed at 81.48 °, 77.24 °, 64.4 °, 44.24 °, and 38.04 °, that are corresponding to 222, 311, 220, 200 and 111 planes, respectively. It was observed that the crystalline phase of the formed AgNPs was cubic and for determining the lattice constant value, we used one of the previously reported methods [36]. The mean value of lattice constant was calculated to be 4.0904 Å, which is in agreement with the previously reported analysis [37]. The size of the crystallite was determined with the help of earlier reported process and was noticed to be 15 nm [38, 39].

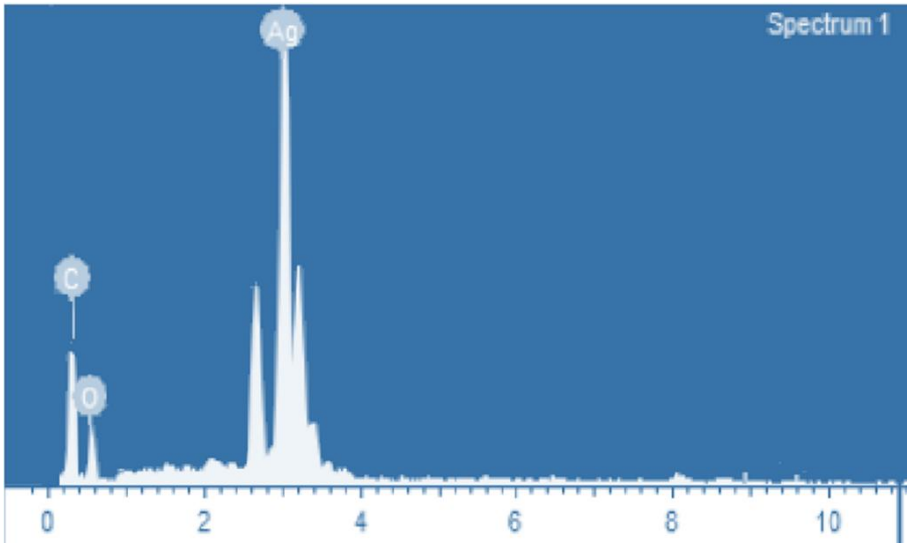

Fig.2. EDS spectrum of prepared AgNPs

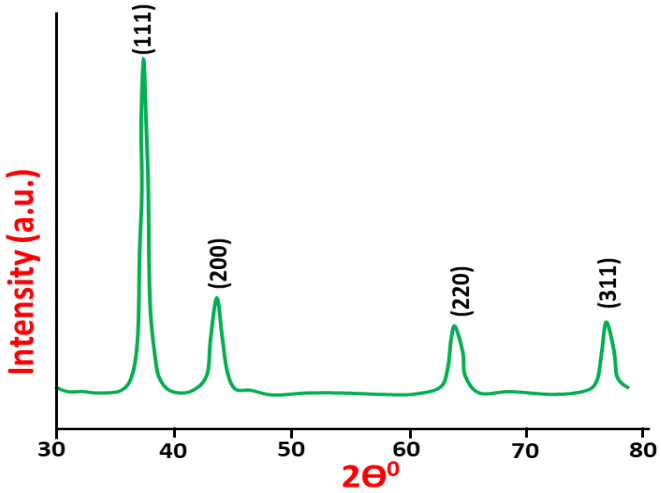

Fig.3. XRD pattern of AgNPs

In addition, surface and size morphologies were observed from the TEM assessment and it was found that both kinds of AgNPs were in spherical form (Fig.

4A, B). The sizes of the formed AgNPs varied from 10 to 15 nm respectively. The size of the formed Ag NPs obtained from the analysis of TEM complied with the size of crystallite evaluated from the XRD spectroscopy.

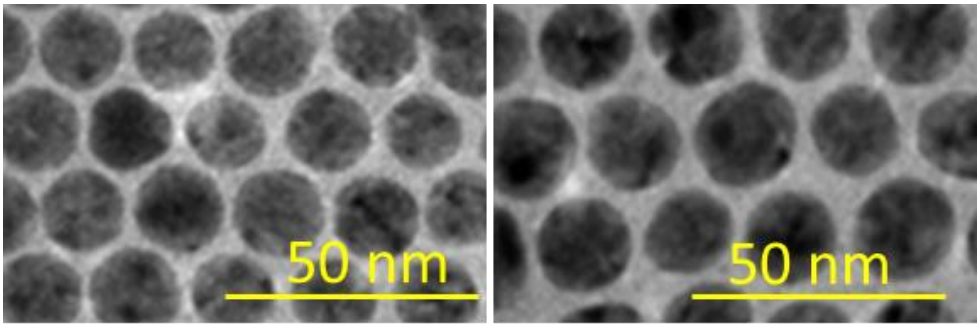

Fig.4. TEM images of AgNPs

Eventually, the functional groups existing in the plant material of *Salvia spinosa* and AgNPs were revealed in the FT-IR spectroscopy (Fig. 5). The presence of 1072.23 cm^{-1} strong band corresponds to the C–O–C or C=O stretches and the band at 1634.38 cm^{-1} inferred to the stretch –C=C. The bands present of 2361.41 and 1800 cm^{-1} represents the groups −C≡C and −C=O, respectively. The existence of 630 cm^{-1} weak peak and 3409.53 cm^{-1} broad peak correspond to the groups C–H and –NH, respectively [40].

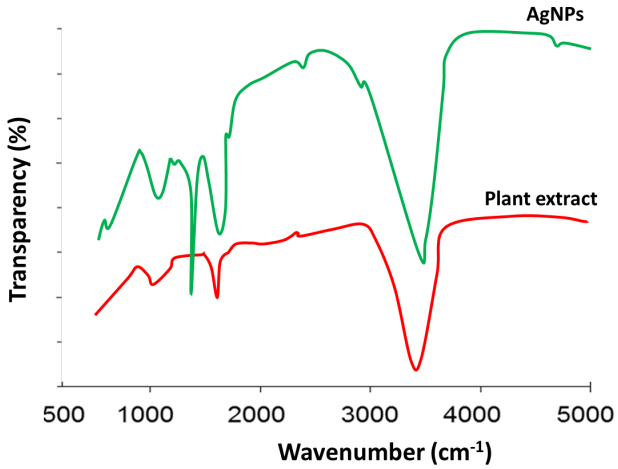

Fig.5. FTIR spectrum of biofabricated AgNPs

Impact of AgNPs on foot pad swelling and Arthritic index

The severity of the disease can be known by the thickness of foot pad and arthritis index (Fig. 6A, B) and they are also utilized to assess the effectiveness of the treatment. CIA induced rats showed a significant increase in the thickness of footpad and AI and this can be demonstrated by the joint swelling, oedema and erythema in ankles and paws. When related to the rats treated with CIA, AgNPs injected rats displayed a decreased inflammation as well as decreased foot pad oedema and erythema where ($p<0.05$). We observed a positive correlation among the changes in the volume of paw oedema and arthritic score.

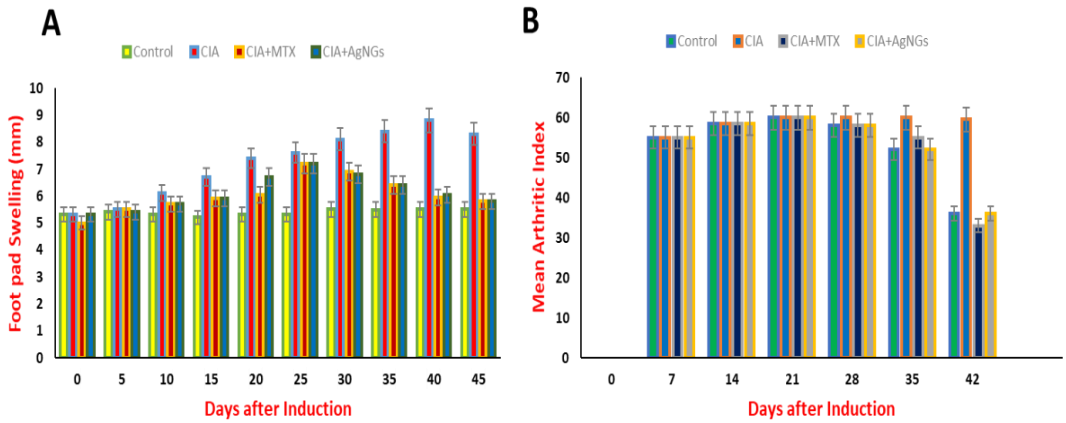

Fig.6. Effect of concentration of AgNPs on (A) foot pad swelling along with (B) arthritic index

Effect of AgNPs on inflammatory mediators

We recorded the TNF-α and IL-1β (Fig. 7A, B) serum levels in CIA induced rats to evaluate the ameliorating impacts of AgNPs on the development of pro-inflammatory cytokines, which is accountable for cartilage devastation and joint inflammation. In CIA injected rats, we observed an obvious increase in the pro-inflammatory cytokines, IL-1β and TNF-α serum levels (Fig. 7). On treating AgNPs, we observed an obvious reduction in the proinflammatory cytokines, IL-1β (50.76%) and TNF-α (51.21%) levels when related with the CIA treated animals (where $p<0.05$), and therefore these findings were similar to those of the target medication (MTX)-administrated rats.

AgNPs effect on COX-2 and NF-kB levels

In CIA treated animals, the COX-2 and NF-kB levels functionality was observed to be significantly greater than that of the control group (Fig. 7C, D). Decrease in the levels of COX-2 (53.80 percent) and NF-kB (47.42 percent) activity was viewed in the animals treated with AgNPs and therefore these findings were similar to those of MTX-administrated drugs.

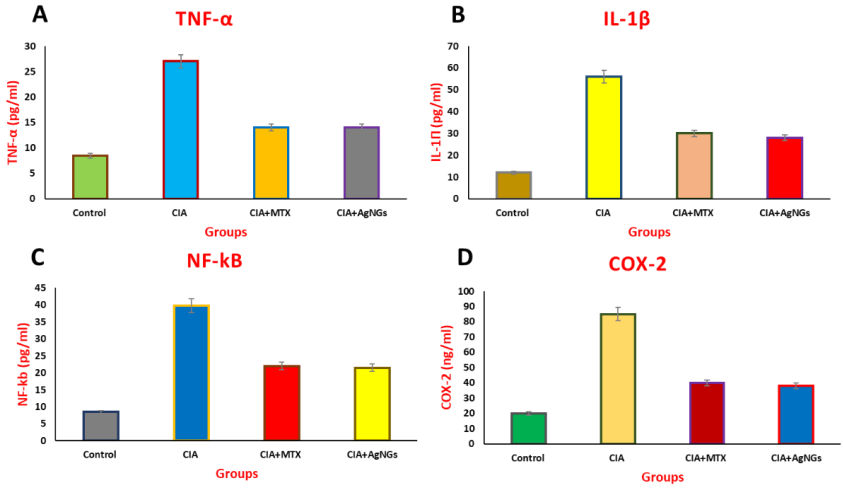

Fig.7. AuNPs effect on (A) TNF-a, (B) IL-1b, (C) NF-kB and (D) COX-2.

AgNPs effect on oxidative damages induced by CIA

In CIA induced rats' serum, we measured the levels of GSH and MDA in order to evaluate the impacts of AgNPs on the damage of oxidative tissue caused by the CIA. Oxidation of cellular damage and membrane lipids are caused due to the increased oxidative stress. Higher levels of MDA are a useful measure of lipid peroxidation. The levels of MDA in CIA induced rats serum were noticed to be raised substantially, but on treating with AgNPs, the levels of MDA got decreased (Fig. 8A) (where $p<0.05$). The decreased levels of GSH in CIA induced rat's entire blood also got retrieved after treating with AgNPs. Therefore, these results have shown that AgNPs administration decreases oxidative damage induced by CIA and these findings are similar to those of the MTX group (Fig. 8B).

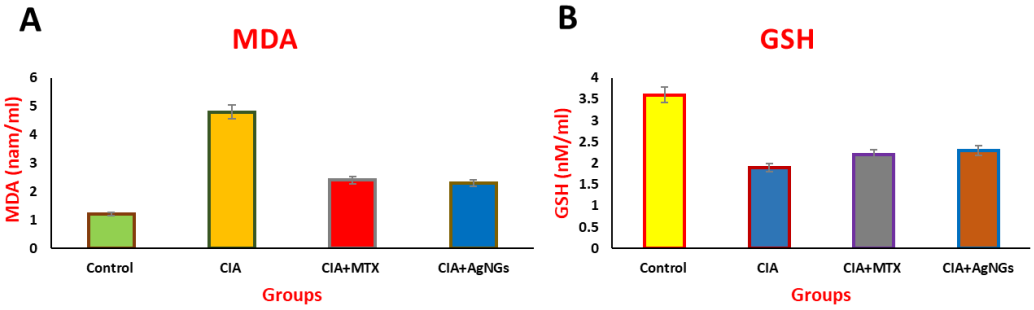

Fig.8. AgNPs effect on (A) MDA, (B) GSH.

AgNPs effect on TNF-a, NF-kB, iNOS and COX-2 mRNA expression

We analyzed the NF-kB, TNF-α, iNOS and COX-2 mRNA expression levels with the help of qPCR in order to evaluate the inhibitory influence of AgNPs on the ROS / RNS and other acidic mediators in the animal groups induced with CIA (Fig. 9A-D). In CIA induced rats, COX-2, TNF-α, iNOS, and NF-kB expression levels were noticed to be considerably improved when compared to healthy control group rats. Furthermore, these upregulations were significantly inhibited post treating with AgNPs (Fig. 9). When related to CIA induced rats, the activity of these inflammatory intermediates reduced considerably on treating with both AgNPs and MTX drug (where $p<0.05$). Therefore, these findings show that the decrease in the transcriptional levels of COX-2, TNF-α, iNOS, and NF-kB expression led to AgNPs inhibition impact on the generation of ROS and inflammatory cytokines.

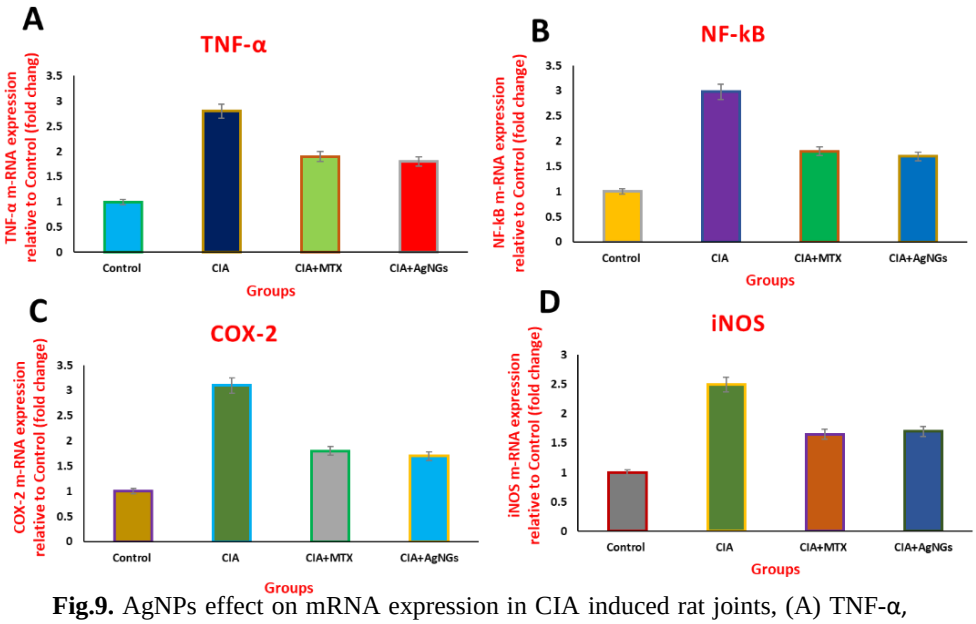

Fig.9. AgNPs effect on mRNA expression in CIA induced rat joints, (A) TNF-α, (B) NF-kB, (C) COX-2, and (D) iNOS.

AgNPs effect on joint tissue histopathology

Histological results of joint tissues with the help of H and E disclosed a huge infiltration of vascular neurons, pannus development and devastation of articular cartilage in animals treated with CIA as a result of persistent molecular and biochemical changes (Fig. 10A–D). Treating with AgNPs has considerably improved the modifications at the histological level followed by reduced cell influx and bone / cartilage injury.

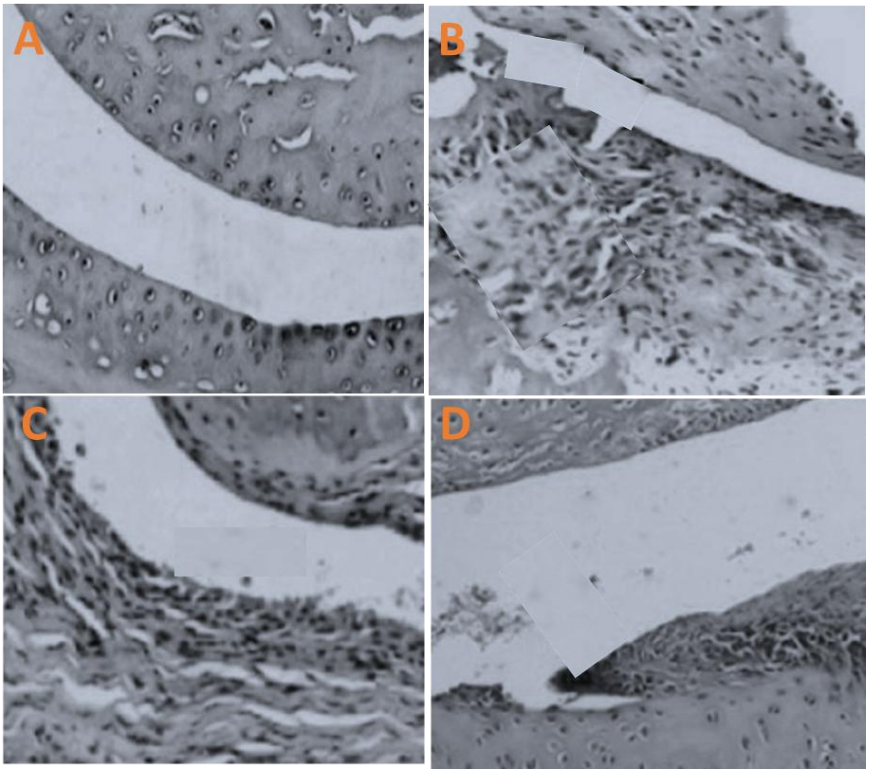

Fig.10. Histological examination of knee joints in rats. Control rats (A), CIA treated rats (B), MTX treated rats (C) and AgNPs treated rats (D)

Conclusions

In conclusion, AgNPs were successfully synthesized using the leaf extract of *Salvia spinosa*, which served as both a capping and reducing agent. The antiarthritic efficacy of these AgNPs was evaluated in a CIA animal model, revealing a significant reduction in oxidative stress and inflammatory mediators. AgNPs demonstrated a marked decrease in the levels of key inflammatory markers, including NF-κB, COX-2, TNF-α, and IL-1β, which were notably elevated in CIA-induced rats. Furthermore, the imbalance between oxidants and antioxidants was assessed, and treatment with AgNPs significantly restored this balance toward normal physiological levels.

Consistent with the biochemical findings, mRNA expression levels of NF-κB, TNF-α, iNOS, and COX-2 were found to be upregulated in CIA-induced rats, whereas AgNP treatment led to their significant downregulation. These molecular outcomes were corroborated by histological analysis of joint tissues, which revealed reduced inflammation and bone erosion in AgNP-treated animals. Overall, the present study highlights the therapeutic potential of AgNPs in mitigating oxidative

stress and inflammatory responses in CIA-induced arthritis, suggesting their promising application in joint repair and antiarthritic interventions

Funding
This work was supported by PhD start-up fund (24BSQD48), Teaching Reform Research Project of Regular Higher Education Institutions in Hunan Province (HNJG-20230917), the First Basic Education Teaching Reform Research Project in Hunan Province (Y20230619).

Data availability
The data associated with the findings of this study are available from the corresponding authors, upon reasonable request.

Conflict of interest
All the authors have declared that no conflict of interest related to this work.

Ethical statement
This research was carried out in line with the principles and standards outlined in the institutional Committee on Ethics of Animal Experimentation. All the animal experiments were performed according to ethical committee guidelines of Hunan University of Arts and Science, Changde 415000, Hunan, China.

References
[1] Vignesh S, Rajaganapathy K, Parthasarathi V, Manikandan K, Hemalatha S, Vibhanshu Raj, Srinivasan R, Regulatory Role of Inflammatory and Pro-Inflammatory Cytokines in Rheumatoid Arthritis: Mechanisms and Therapeutic Insights, *Int. J. of Pharm. Sci*, 2025; 3 (6), 2036-2047. DOI: 10.5281/zenodo.15634070
[2] Murayama MA, Shimizu J, Miyabe C, Yudo K and Miyabe Y. Chemokines and chemokine receptors as promising targets in rheumatoid arthritis. *Front. Immunol.* 2023; 14:1100869. DOI: 10.3389/fimmu.2023.1100869
[3] Nanki T, Imai T, & Kawai S. Fractalkine/CX3CL1 in rheumatoid arthritis. *Modern Rheumatology*, 2016; 27(3), 392–397. DOI: 10.1080/14397595.2016.1213481
[4] Lark MW, Bayne EK, Flanagan J, Harper CF, Hoerrner LA, Hutchinson NI, Singer II, Donatelli SA, Weidner JR, Williams HR, Mumford RA, Lohmander LS. Aggrecan degradation in human cartilage. Evidence for both matrix metalloproteinase and aggrecanase activity in normal, osteoarthritic, and rheumatoid joints. *J Clin Investig*. 1997; 100, 93–106. DOI: 10.1172/JCI119526
[5] Anilkumar S, Wright-Jin E. NF-κB as an Inducible Regulator of Inflammation in the Central Nervous System. *Cells*. 2024; 13(6):485. DOI: 10.3390/cells13060485
[6] Hoffmann A, Cheng G. & Baltimore D. NF-κB: master regulator of cellular responses in health and disease. *Immun. Inflamm.* 2025; 1. DOI: 10.1007/s44466-025-00014-0

[7] Dejardin E. The alternative NF-kappaB pathway from biochemistry to biology: pitfalls and promises for future drug development. *Biochem Pharmacol*. 2006; 72, 1161–1179. DOI: 10.1016/j.bcp.2006.08.007
[8] Seeger DR, Cosalich DDB, Smith JM, Hultquist MA. Analogs of Pteroylglutamic Acid. VI. 3',5'-Dihalopteroyl Derivatives. *J Am Chem Soc.* 1949;71, 1297–1301. DOI:10.1021/JA01150A041
[9] Zhang Y, Chen L, & Kumar A. Resolution of inflammation in rheumatoid arthritis: Cellular mechanisms and therapeutic implications. *Frontiers in Cell and Developmental Biology*, 2025; *13*, 1556359. DOI:10.3389/fcell.2025.1556359
[10] Rohitas D. Rheumatoid arthritis: Pathophysiology, current therapeutic strategies and recent advances in targeted drug delivery system. *Materials Today Communications*, 2023; 35, 105877. DOI: 10.1016/j.mtcomm.2023.105877.
[11] Scott DL, Kingsley GH. Tumor Necrosis Factor Inhibitors for Rheumatoid Arthritis. *N Engl J Med*. 2006; 355, 704–712. DOI: 10.1056/NEJMct055183
[12] Malik S, Muhammad K, & Waheed Y. Nanotechnology: A Revolution in Modern Industry. *Molecules (Basel, Switzerland)*, 2023; *28*(2), 661. DOI: 10.3390/molecules2802066
[13] Zhang Y, and Wang J. Nanoscale materials: Surface properties and reactivity. *Nano*, 2023; 18(3), e202300038. DOI: 10.1002/nano.202300038
[14] Shams S, Martinez JM, Dawson JRD, Flores J, Gabriel M, Garcia G, et al. The therapeutic landscape of rheumatoid arthritis: current state and future directions. *Front Pharmacol*. 2021;12: 680043. DOI: 10.3389/fphar.2021.680043.
[15] Warnasooriya N, Joud F, Bun P, Tessier G, Coppey-Moisan M, Desbiolles P, Atlan M, Abboud M, Gross M. Imaging gold nanoparticles in living cell environments using heterodyne digital holographic microscopy. *OpticsExpress*. 2010; 18, 3264–3273. DOI: 10.1364/OE.18.003264
[16] Burlec AF, Corciova A, Boev M, Batir-Marin D, Mircea C, Cioanca O, Danila G, Danila M, Bucur A.F, Hancianu M. Current Overview of Metal Nanoparticles' Synthesis, Characterization, and Biomedical Applications, with a Focus on Silver and Gold Nanoparticles. *Pharmaceuticals*, 2023; *16*, 1410. DOI: 10.3390/ph16101410
[17] Patel J, Kumar G.S, Roy H. *et al.* From nature to nanomedicine: bioengineered metallic nanoparticles bridge the gap for medical applications. *Discover Nano*, 2024; 19, (85). DOI: 10.1186/s11671-024-04021-9
[18] Eben B, Shajan A, Elessy A. Role and Biomedical Application of metal nanoparticles in cancer immunotherapy. *International Journal of Research Publication and Reviews*, 2025; 6 (5), 11470-11472
[19] Tuli H.S, Joshi R, Kaur G. *et al.* Metal nanoparticles in cancer: from synthesis and metabolism to cellular interactions. *J Nanostruct Chem*, 2023; 13, 321–348. DOI: 10.1007/s40097-022-00504-2
[20] Liu X, Dai Q, Austin L, Coutts J, Knowles G, Zou J, Chen H and Huo Q. A one-step homogeneous immunoassay for cancer biomarker detection using gold nanoparticle probes coupled with dynamic light scattering. *Journal of the American Chemical Society*, 2008;130 (9), 2780-2782. DOI: 10.1021/ja711298b

[21] Yun Z and Wei J. Trends in the application of metal Nanobiomaterials in cancer therapy clinical trials. *Front. Nanotechnol.* 2024; 6:1507484. DOI: 10.3389/fnano.2024.1507484
[22] El-Sayed IH, Huang X, & El-Sayed MA. Surface plasmon resonance scattering and absorption of anti-EGFR antibody conjugated gold nanoparticles in cancer diagnostics: applications in oral cancer. *Nano letters*, 2005; 5(5), 829–834. DOI:10.1021/nl050074e
[23] Yang SZ, Liu QA, Liu YL. *et al.* Recent progress in the optical detection of pathogenic bacteria based on noble metal nanoparticles. *Microchim Acta*, 2021; 188, 258. DOI: 10.1007/s00604-021-04885-z
[24] Golchin K, Golchin J, Ghaderi S, Alidadiani N, Eslamkhah S, Eslamkhah M, Davaran S, & Akbarzadeh A. Gold nanoparticles applications: from artificial enzyme to drug delivery. *Artificial cells, nanomedicine, and biotechnology*, 2008; *46*(2), 250–254. DOI: 10.1080/21691401.2017.1305393
[25] Sharma AR, Lee YH, Bat-Ulzii A. *et al.* Recent advances of metal-based nanoparticles in nucleic acid delivery for therapeutic applications. *J Nanobiotechnol*, 2022; (20) 501. DOI: 10.1186/s12951-022-01650-z
[26] Daraee H, Eatemadi A, Abbasi E, Fekri Aval S, Kouhi M, & Akbarzadeh A. Application of gold nanoparticles in biomedical and drug delivery. *Artificial cells, nanomedicine, and biotechnology*, 2016; *44*(1), 410–422. DOI: 10.3109/21691401.2014.955107
[27] Zhengab M, Jiaab H, Wangab H, Liua L, Zhesheng H, Zhanga Z, Yang W, Gaoc L, Gao X, and Fuping G. Application of nanomaterials in the treatment of rheumatoid arthritis. *RSC Adv*, 2021; 11, 7129-7137
[28] Thakor AS, Jokerst J, Zavaleta C, Massoud TF, & Gambhir SS. Gold nanoparticles: a revival in precious metal administration to patients. *Nano letters*, 2011; *11*(10), 4029–4036. DOI: 10.1021/nl202559p
[29] Campo GM, Avenoso A, Campo S. *et al.* Differential effect of growth factors on hyaluronan synthase gene expression in fibroblasts exposed to oxidative stress. *Biochemistry Moscow*, 2007; 72, 974–982. DOI: 10.1134/S0006297907090088
[30] Maleitzke T, Weber J, Hildebrandt A, Dietrich T, Zhou S, Tsitsilonis S, Keller J. Standardized protocol and outcome measurements for the collagen antibody-induced arthritis mouse model.
STAR Protocols, 2022; 3 (4), 101718. DOI: 10.1016/j.xpro.2022.101718.
[31] Satoh K. Serum lipid peroxide in cerebrovascular disorders determined by a new colorimetric method. *Clinica chimica acta; international journal of clinical chemistry*, 1978; *90*(1), 37–43. DOI: 10.1016/0009-8981(78)90081-5
[32] Tietze F. Enzymic method for quantitative determination of nanogram amounts of total and oxidized glutathione: Applications to mammalian blood and other tissues. *Anal Biochem.* 1969; 27, 502–522. DOI: 10.1016/0003-2697(69)90064-5
[33] Hyc A, Osiecka-Iwan A, Dziunycz P, Moskalewski S. Preparation of rat synovial membrane for studies of cytokine secretion. *Folia Histochem Cytobiol.* 2007; 45, 57–60.

[34] Xiayu R, Dejian L, Xuelin H. A New Method for Quantitative Real-Time Polymerase Chain Reaction Data Analysis. *Journal of Computational Biology*, 2013; 20 (9), DOI: 10.1089/cmb.2012.0279
[35] Hasanova G, Omarova S, Khalilov R, Mammadova A, Zafar M, Salman Majeed, Mohamed Fawzy Ramadan, Muhammad Rizwan Khan, Aleena Gul. Artemisia lerchiana Based Green Synthesis of Silver Nanoparticles: TEM Microscopy, Physicochemical, and Spectroscopic Characterization. *Microscopy research and technique, 2025;* DOI: 10.1002/jemt.70062
[36] Disha P, Bhakti P, Virendra Kumar Y, Sudhakar M.P, Ali Alharbi S, Salmen S.H, Illa P, Nisha C, Ashish P. Silver nanoparticles synthesized from marine algae Spatoglossum asperum: Antioxidant properties and seed germination enhancement. *Journal of Hazardous Materials Advances.* 2024; 16, 100478. DOI: 10.1016/j.hazadv.2024.100478.
[37] Gecer EN, Erenler R, Temiz C, Genc N, & Yildiz I. Green synthesis of silver nanoparticles from *Echinacea purpurea* (L.) Moench with antioxidant profile. *Particulate Science and Technology*, 2021; *40*(1), 50–57. DOI:10.1080/02726351.2021.1904309
[38] Wasan A. Al-Dulaimi, Zeena M. Al-Azzawi, Emad K. Al-Shakarchi. A Pioneering Approach to the Synthesis of Silver Nanoparticles.2024; 12(7). DOI: DOI: 10.4236/msce.2024.127002
[39] Alam HMB, Das R, Shajahan M, Ullah AKMA, Kibria AKMF. Surface characteristics and electrolysis efficiency of a Palladium-Nickel electrode. *Int. J. Hydrog*. 2018; Energy 43, 1998–2008. DOI: 10.1016/j.ijhydene.2017.12.027
[40] Yang F, Zhao M, Zheng B, Xiao D, Wu L, Guo Y. Influence of pH on the fluorescence properties of graphene quantum dots using ozonation pre-oxide hydrothermal synthesis. *J. Matter. Chem*. 2012; 22, 25471–25479. DOI: 10.1039/C2JM35471C